Crystallization of Ge and Si in metal films. I*

G. Ottaviani, D. Sigurd, V. Marrello, J. W. Mayer, and J. O. McCaldin

California Institute of Technology, Pasadena, California 91109
(Received 4 June 1973; in final form 4 September 1973)

The behavior of amorphous Si in contact with Ag films and Ge in contact with Al films has been studied at temperatures well below those at which any liquid phase is present. MeV $^4He^+$ ion backscattering techniques, transmission electron diffraction, scanning electron microscopy, and electron microprobe analysis have been used. We find that of the many possible reactions which carry the amorphous Si or Ge into their crystalline forms the reaction predominating under our experimental conditions consists of dissolution, diffusion, and crystal growth. During isothermal heat treatment, the semiconductor film is dissolved into the metal film where it diffuses and precipitates as crystalline Si or Ge. These processes are solid-solid reactions, since this behavior is observed over temperatures of 300°C to as low as 100°C for Ge/Al, compared to the 424°C eutectic in this system. In Si/Ag, this behavior was observed from 700 to 400°C, compared with the 840°C eutectic.

I. INTRODUCTION

Electrical contacts to semiconductor devices are formed by evaporating metal layers and heat treating. Consequently, metal-semiconductor interfaces and reactions play dominant roles in these metallization processes. With the standard Al metallization on Si, it has been found that Si dissolves in Al during forming of the contacts to a sufficient extent that severe erosion occurs.[1,2] To overcome this erosion, commercial practice often entails coevaporation of Si to suppress the dissolution reaction.

Another approach is to evaporate a layer of Si on top of the aluminum. Upon heat treatment, the Si migrates into the Al and suppresses the erosion. However, undesirable Si precipitates are sometimes formed.

There has also been considerable interest recently in the behavior of amorphous Si and Ge in contact with metal films. It has been found that crystallization of the amorphous semiconductor layers occurs at significantly lowered temperatures when the amorphous layer is in contact with a metal as compared with a single-crystal substrate of the same semiconductor.[3-7] For Si, the crystallization temperature is 600–700 °C and is lowered to 300–540 °C when the Si is in contact with Ag. Germanium has been found to crystallize at 400 °C and when Ge is in contact with Al at 120–210 °C. The same phenomena occur for amorphous layers formed by vacuum deposition or by ion implantation. The mechanism leading to this lowered crystallization temperature has been interpreted as being due to mass transport at the interface between films[5] or to a lowering of the apparent binary eutectic temperature.[8]

We have previously studied the behavior of single-crystal semiconductors in contact with metals. We have found that dissolution and transport of the semiconductor take place in the metal at temperatures well below that at which any liquid phase exists. One striking example[9] is the transport of large amounts of Si through Au films to form SiO_2 layers at temperatures of 100–200 °C. Another example is that studies of dissolution and migration of Si in Al films indicate an enhancement of diffusivity by as much as $1\frac{1}{2}$ orders of magnitude.[2] The enhancement in diffusivity was not accompanied by a measurable enhancement of solubility over values for Si in wrought Al. Similarly, single-crystal Ge in contact with evaporated Al films was found to saturate the solid Al film with dissolved Ge at temperatures well below that of the eutectic.[10]

Precipitation and epitaxial regrowth have been found to occur in structures consisting of single-crystal Ge or Si covered with an Al film.[11,12] Upon heating, the Al film is saturated with Si or Ge and, upon cooling, the dissolved semiconductor becomes supersaturated. If the supersaturated semiconductor is within about a diffusion length of the single-crystal–metal interface, the supersaturation can be relieved by epitaxial growth. If on the other hand the interface is far away, precipitates of the semiconductor are formed within the Al matrix.[13]

The nucleation and growth of precipitates out of a supersaturated solution is a familiar process.[14] The precipitate growth ordinarily occurs upon cooling. In contrast, the formation of precipitates occurs at constant temperature for amorphous layers of Ge and Si in contact with metal films. In a previous note[15] we proposed that the formation of crystalline precipitates proceeds through the following steps: (i) dissolution of the semiconductor by the the metal film, (ii) transport to a nucleation site, and (iii) subsequent growth of crystallites. We speculated that this crystallite formation was possible at constant temperature due to the higher free energy of amorphous semiconductors, as compared to that of single crystals.

Since the amorphous material transforms into crystalline material when kinetics permit, clearly the amorphous material has higher free energy than does the crystal material. Consequently, the concentration of solute Si dissolving into the metal solvent from amorphous material will be higher than if dissolution were occurring from crystalline material. In dilute solutions the concentration of solute is proportional to $\exp(\overline{G}/kT)$, where $\overline{G}$ is the free energy per solute atom. Therefore, the excess free energy $\Delta\overline{G}$ associated with the amorphous material in contact with the solvent should enhance solute concentrations.

The purpose of the present work is to investigate in more detail the crystallization of Si in Ag films and Ge in Al films. These two systems were chosen as representative of simple eutectic behavior (the Ge/Al eutectic is 424 °C, and the Si/Ag is 840 °C). In all cases we kept the process temperature more than 100 °C below the eutectic temperature to prevent the formation of liquid phases. The work appears in two parts. In this paper (I) we discuss the formation of the precipitates. In the accompanying paper (II)[16] we describe the crystalline nature of the precipitates.

II. SPECIMEN PREPARATION AND ANALYSIS

Specimens for this investigation were prepared by vacuum deposition of Ag, Al, Ge, and Si onto substrates of Ge, Si, and in a few cases vitreous carbon. One side of the Ge and Si wafers was polished, and the following procedure was used to clean the surface before evaporation. The wafers were etched in CP_4 for ~30 sec and were afterwards quenched in deionized water. Then the samples were immersed in a dilute solution of HF and were removed just before loading into the evaporation chamber. The evaporation system used utilized an e-gun evaporator, and the system was pumped by an ion pump. This gives a pressure of $(2-5)\times 10^{-7}$ Torr during evaporation. The geometry of the system is such that the samples, held at ambient temperature, are mounted ~20 cm above the source. At roughly the same height, a quartz oscillator thickness monitor is located. For all elements used, the rate of deposition was 10–40 Å/sec, monitored by the quartz oscillator. These evaporation conditions have been shown to produce amorphous layers of Si and Ge.[17,18] This was confirmed for our films by transmission electron diffraction. Immediately after unloading of the evaporation system, the samples were heat treated for times ranging from 5 min to 20 h in a quartz tube furnace with a dry N_2 atmosphere. After heat treatment, samples were pulled out of the furnace to obtain a fast cooldown.

Two sequences of evaporation were used: either substrate/metal/semiconductor or substrate/semiconductor/metal. The range of thicknesses used were between 3000 and 5000 Å for Al and between 50 and 2000 Å for Ge. The Si thicknesses ranged from 300 to 2000 Å and the Ag films were between 1600 and 3000 Å thick. The actual thicknesses of the films were measured by backscattering of MeV $^4He^+$ ions (see Sec. III). This technique gives thickness values in atoms/cm^2. For convenience, we assume bulk density and give thicknesses in angstroms. The samples were studied by four different techniques: MeV $^4He^+$ ion backscattering, scanning electron microscopy, electron microprobe analysis, and transmission electron diffraction. Backscattering measurements were made using 2-MeV $^4He^+$ ions from the Kellogg 3-MV accelerator.[19] Particles scattered from the target in a 168° laboratory angle were monitored by a surface barrier detector. The energy resolution of the electronic system was 18–20 keV.

Backscattering measurements give the distribution of elements as a function of depth within the sample. To obtain the lateral distribution, scanning electron microscopy (SEM) and electron microprobe analysis were used. For SEM techniques etching and cleaning of the samples were required in some cases. The Al and Ag were etched by dilute sodium hydroxide and dilute ferric nitrate, respectively. To obtain lateral views of the structures, samples were cleaved in liquid nitrogen to avoid smearing of the metal. For electron microprobe studies of lateral distribution of the semiconductor in the metal film, it is necessary to avoid interference from the underlying substrate. For the films studied in this work some contribution from the substrate was found even at the lowest electron energy used (4 keV). This energy corresponds to roughly 5000-Å penetration depth. The substrate interference could be eliminated by using carbon substrates for the Si/Ag structures and carbon or Si substrates for the Ge/Al films.

For transmission electron studies the composite film was removed from the substrate with Scotch tape. This was successful only for Si/Ag film on carbon substrates and Ge/Al on Si. This work is reported in paper II.

III. BACKSCATTERING ANALYSIS

Backscattering measurements give information on the distribution of mass in depth. Analysis of energy distributions of backscattered particles is straightforward when the targets are laterally uniform. However, if the target is laterally nonuniform in either thickness or composition, the spectra give averages across lateral dimensions of the beam spot (~1–2 mm). In spite of this, detailed analysis of widths of peaks in the spectra can often give qualitative information on the lateral distribution. Further identification of the target can be provided by SEM or electron microporbe analysis.

Figure 1(a) shows a schematic spectrum for a carbon

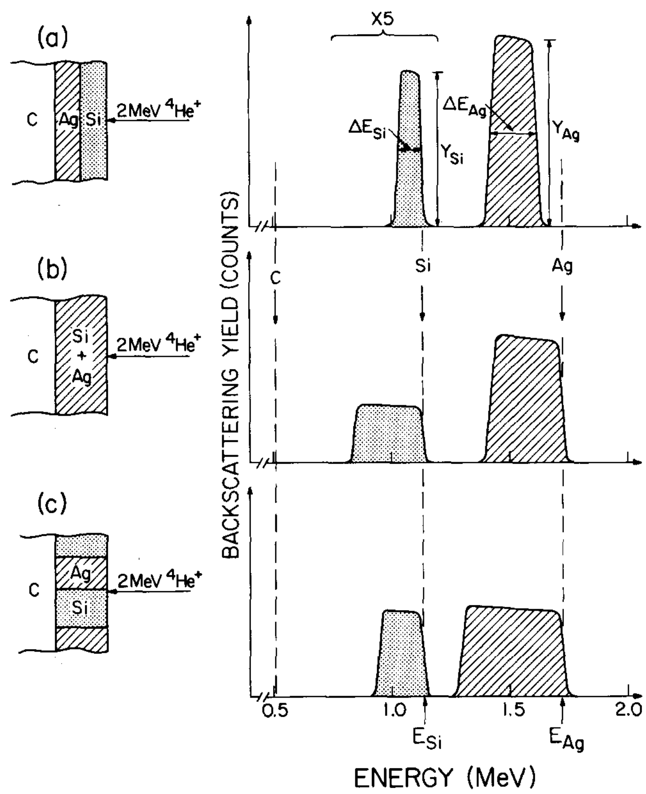

FIG. 1. Schematic energy spectra for 2-MeV $^4He^+$ ions backscattered from equal numbers of Si and Ag atoms/cm^2 in composite structures on carbon substrates. (a) Spectrum for a Si film deposited on a Ag film; (b) spectrum for a uniform mixture; (c) spectrum for elemental islands.

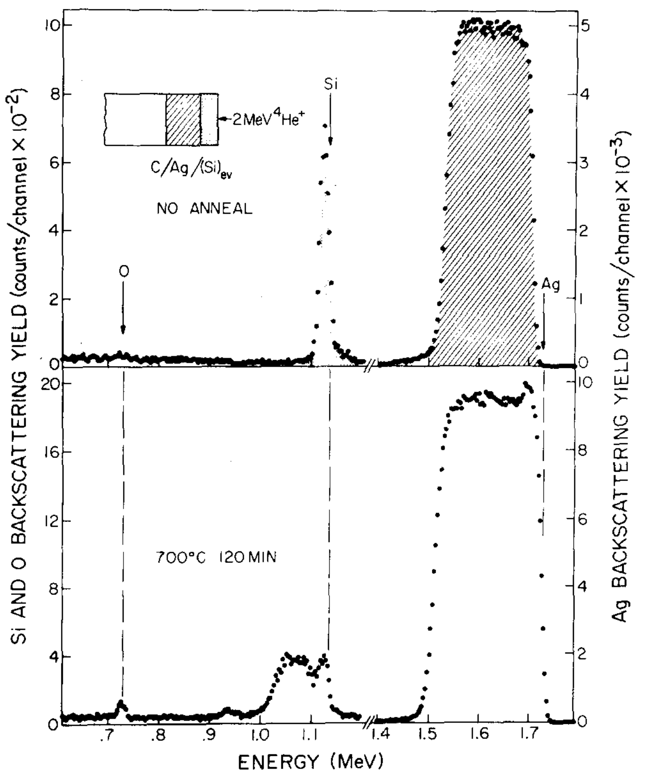

FIG. 2. Backscattering spectra for 2-MeV ^{4}He incident on a 370-Å Si layer evaporated on a 1670-Å Ag layer deposited on a carbon substrate. The upper portion of the figure shows the as-deposited case with the Ag component shaded and the Si component dotted. The lower portion shows the spectrum after annealing at 700 °C for 120 min. In this figure the arrows indicate the energy corresponding to scattering from atoms at the surface.

substrate covered with equal numbers of Ag and Si atoms per cm^2. Arrows on the energy axes denote the energy positions corresponding to scattering from atoms on the surface. The Ag component of the spectrum is shifted below its surface position owing to energy loss of the He projectiles on their inward and outward trajectories through the overlying Si layer. The carbon component is also shifted to lower energies and is omitted for the sake of clarity. The widths of Si (ΔE_{Si}) and Ag (ΔE_{Ag}) components reflect the difference in stopping power of He ions in the different materials: $\Delta E_{Si}/\Delta E_{Ag} = 0.44$. For film thicknesses of a few thousand angstroms, the widths ΔE of the signals are nearly proportional to the film thickness; there is only a 5% deviation from linearity for a 5000-Å Si layer.[20] The heights Y_{Si} and Y_{Ag} can be calculated from scattering cross sections and stopping powers (see Appendix) to give a ratio $Y_{Ag}/Y_{Si} = 6.50$.

For a target composed of a homogeneous layer of the same amounts of Si and Ag, the Ag and Si components [Fig. 1(b)] are broader and lower in height. The widths are nearly equal ($\Delta E_{Si}/\Delta E_{Ag} = 0.93$) and extend out to the surface position. In this case the ratio of Si to Ag atoms/cm^2 determines the ratio of the heights of the two components.

For a target [Fig. 1(c)] with islands of Si and Ag of equal thickness, the ratio of energy widths is 0.44, the same as that for uniform layers [Fig. 1(a)]. For equal amounts of Si and Ag, the exposed area of Si will be 17% greater than that of Ag owing to differences in density. These area differences are reflected in the heights of the two portions of the energy spectrum.

Figure 2 shows backscattering spectra for a 370-Å Si layer evaporated overlying a 1670-Å-thick Ag layer. The Ag signal is shifted to lower energy owing to the presence of the Si layer. After heat treatment at 700 °C, the nature of the target has changed. The high-energy edge of the Ag has shifted to the surface position, and the Si signal has broadened and decreased. The ratio of the energy widths, 0.52, suggests that islands of Si and Ag are formed. The peak in the leading edge of the Si signal and the appearance of a peak at the position corresponding to that of oxygen show that an oxide layer is formed at the surface. The integrated area of the oxygen signal gives 3×10^{16} O atoms/cm^2, equivalent to a SiO_2 thickness of 70 Å.

Figure 3 shows a backscattering spectrum from a Ge substrate covered with 220 Å of evaporated Ge and 4000 Å of Al. The Al signal appears as a peak superimposed on the Ge signal. The Ge signal is displaced below the surface position owing to the energy loss of the He particles in transversing the Al film.

In Fig. 3 the contribution from the evaporated Ge layer cannot be separated from that of the signal from the Ge substrate. Although it is possible to distinguish the two components by the use of channeling techniques, a

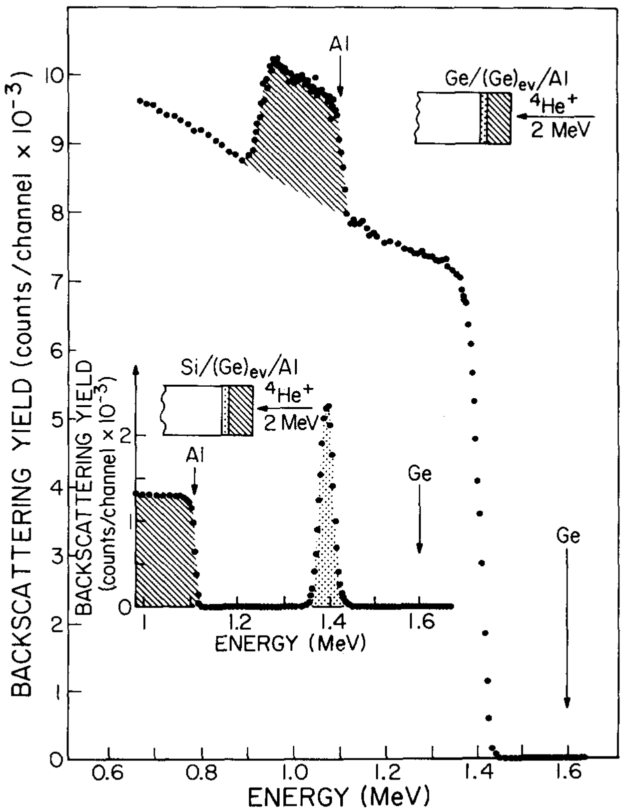

FIG. 3. Spectrum for a Ge substrate covered with 220-Å Ge followed by 4000-Å Al. The insert shows the spectrum from a Si substrate that was adjacent to the Ge substrate during evaporation. The arrows indicate the energy corresponding to scattering from atoms at the surface.

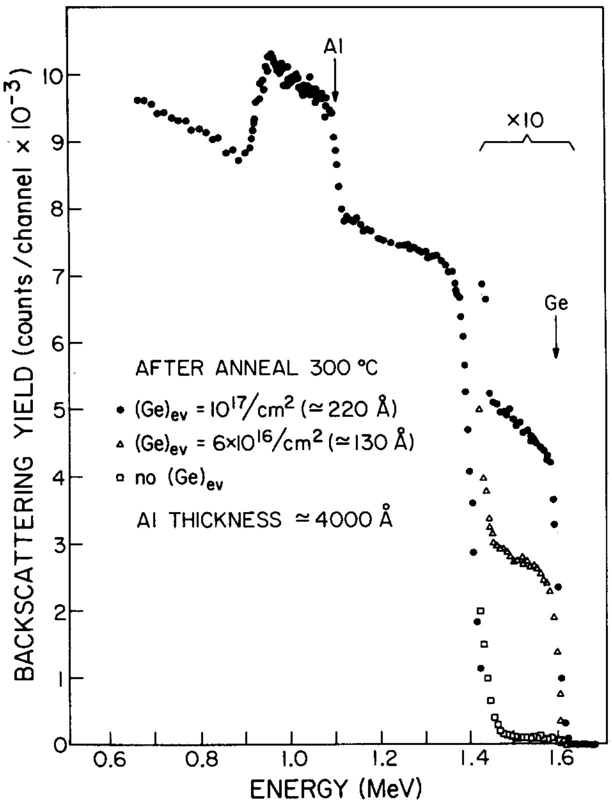

FIG. 4. 2-MeV ^{4}He spectra from Ge/Al structures annealed at 300 °C. The open squares indicate the portion of the samples covered by Al but not with Ge. The arrows indicate the energy corresponding to scattering from atoms at the surface.

simpler method for finding the number of Ge atoms/cm^2 is to evaporate simultaneously on Si and Ge substrates. The inset shows the spectrum for a Si substrate that was placed immediately adjacent to the Ge sample during evaporation. The signal from the Ge layer is now clearly visible. Comparison of the total number of counts on the Ge signal with the heights of the Al signal gives directly the number of Ge atoms/cm^2. For this sample the Ge thickness was 10^{17} atoms/cm^2, which corresponds to 220 Å if bulk density is assumed.

IV. RESULTS AND DISCUSSION

A. Ge/Al

During heat treatment at 100—300 °C, Ge moves into the Al film. This is evident from the backscattering spectra shown in Fig. 4 for two samples annealed at 300 °C. The component due to Ge atoms in the composite film appears in the energy region 1.4—1.6 MeV, the region between the shoulder of the Ge thick-target yield and the energy position corresponding to Ge atoms at the surface (indicated by the arrow). The two samples had different thicknesses of evaporated Ge—130 and 220 Å, respectively, measured on an adjacent Si sample (see Fig. 3). This difference in amounts of evaporated Ge is reflected in the heights of the plateaus arising from the Ge in the heights of the plateaus arising from the Ge in the composite film. Within the accuracy of the backscattering measurements, all the Ge originally evaporated is now present in the composite film. In Fig. 4, the edges of the Al signal are sharp, which indicates that the composite structure is uniformly thick over the

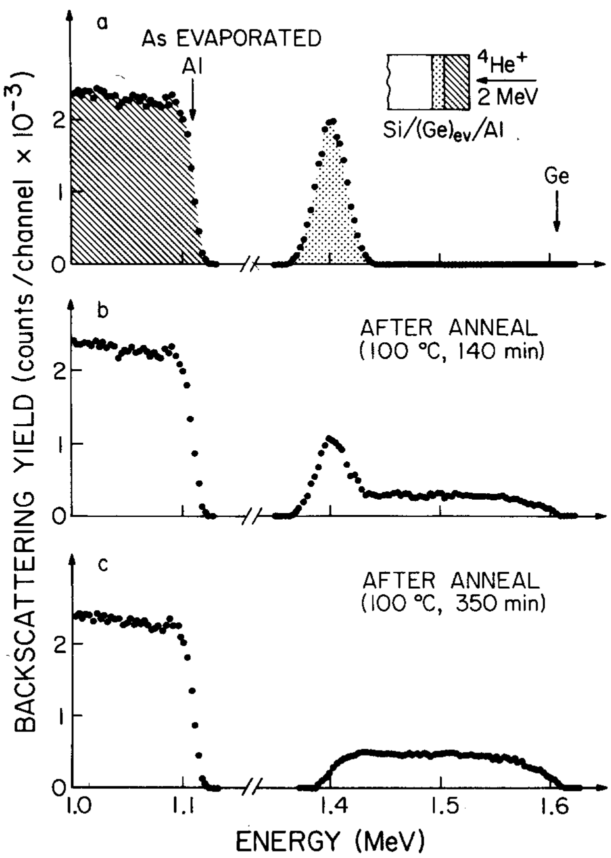

FIG. 5. Spectrum for a 100-Å Ge layer covered by a 4000-Å Al layer on a Si substrate. The arrows show the energy positions for Al and Ge at the surface. The backscattering component from the Si substrate is not visible because components below 1.0 MeV are suppressed.

~2-mm^2 area probed by the analyzing He^+ beam.

In preparation of the samples for Fig. 4, the evaporated areas were masked so that a portion of the sample had only a evaporated layer of Al. Ge from the single-crystal substrate is dissolved into the Al film, which is indicated by the lowest data points (open squares). In this case, however, the amount of Ge in the Al is determined by solid solubility and is ~0.5 at.% at 300 °C.

The motion of Ge into the Al film can be seen more clearly when Si substrates are used. Figure 5(a) shows the backscattering spectrum for a 100-Å Ge layer covered with a 4000-Å Al film. Upon heating the sample at 100 °C for 140 min [Fig. 5(b)], some of the underlying Ge has moved into the Al film. After 350 min [Fig. 5(c)], the Ge is distributed uniformly in depth throughout the composite film structure.

In samples with thicker Ge layers, a uniform distribution of Ge and Al in depth throughout the composite film is not generally observed. Figure 6(a) shows a backscattering spectrum for a Si sample with 1840 Å of Ge and 3600 Å of Al. After heating at 300 °C for 60 min [Fig. 6(b)], the positions of Ge and Al have nearly reversed. The major fraction of Ge is near the surface and the major fraction of Al is in contact with Si. With further heating at 300 °C [Fig. 6(c)] there is a tendancy toward a more uniform distribution in depth with a reduction in the amount of Ge at the surface. The Si-Al

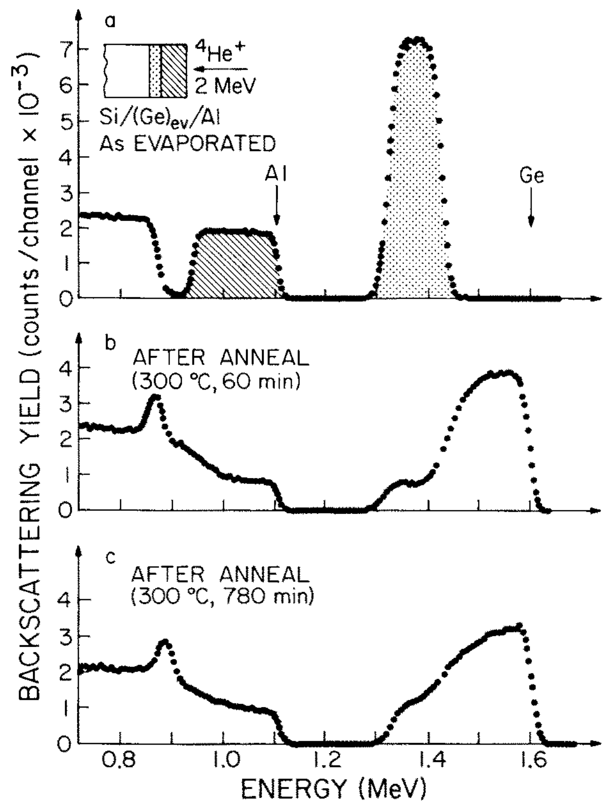

FIG. 6. Spectrum for a 1840-Å Ge layer covered by a 3600-Å Al layer on a Si substrate. In the as-deposited spectrum (a) the Al portion is shaded and is separated from the Si continuum owing to the intervening Ge layer (dotted portion). After annealing at 300 °C (b and c) the Al is in contact with the Si substrate, which results in an overlap peak at 0.88 MeV. The arrows indicate the energy corresponding to scattering from atoms at the surface.

overlap peak at 0.88 MeV is due to the mass difference between Al and Si.[21]

Figures 5 and 6 show that the Ge distribution changes with successive heat treatments. These results as well as those obtained by scanning electron microscopy, indicated below, clearly show that the Ge/Al intermixing predominantly occurs during heat treatment and not during cooling.

SEM pictures were taken of the sample after heating to 300 °C at a position adjacent to the spot analyzed by backscattering. Figures 7(a) and 7(b) show the sample after heating for 1 and 4 h, respectively. The surface has a patched appearance due to the difference in secondary emission of Ge and Al. Electron microprobe analysis indicated that the white areas are Ge and the black are Al. Figure 7 shows, in agreement with backscattering data of Fig. 6, that initially there is a movement of a relatively large amount of Ge to the surface and that the amount of Ge at the surface decreases with prolonged heating. There is also a marked coarsening of the Ge structure with longer heat treatment, which is apparent from Fig. 7.

The amount of Ge contained in the composite films after annealing, measured by backscattering, was orders of magnitude above the solid solubility of Ge in Al. The results of scanning electron micrographs of the surface show that at the surface there are localized regions of Ge in a surrounding Al matrix. Further information was obtained from electron microprobe analysis, which showed that the Ge was in the form of precipitates with lateral sizes of 2000–40 000 Å.

SEM techniques were also used to examine the Ge precipitates on cleaved and etched samples. Figure 8 shows micrographs of a sample with 1840 Å of Ge and 3600 Å of Al after heating at 300 °C for 60 min. The upper micrograph [Fig. 8(a)] of a cleaved surface shows Ge precipitates (appearing as white islands) imbedded in a matrix of Al. The top surface of the composite film is relatively flat. This same sample was etched to remove the Al. The Ge precipitates [Fig. 8(b)] are smooth topped with some indication of undercutting near the Si

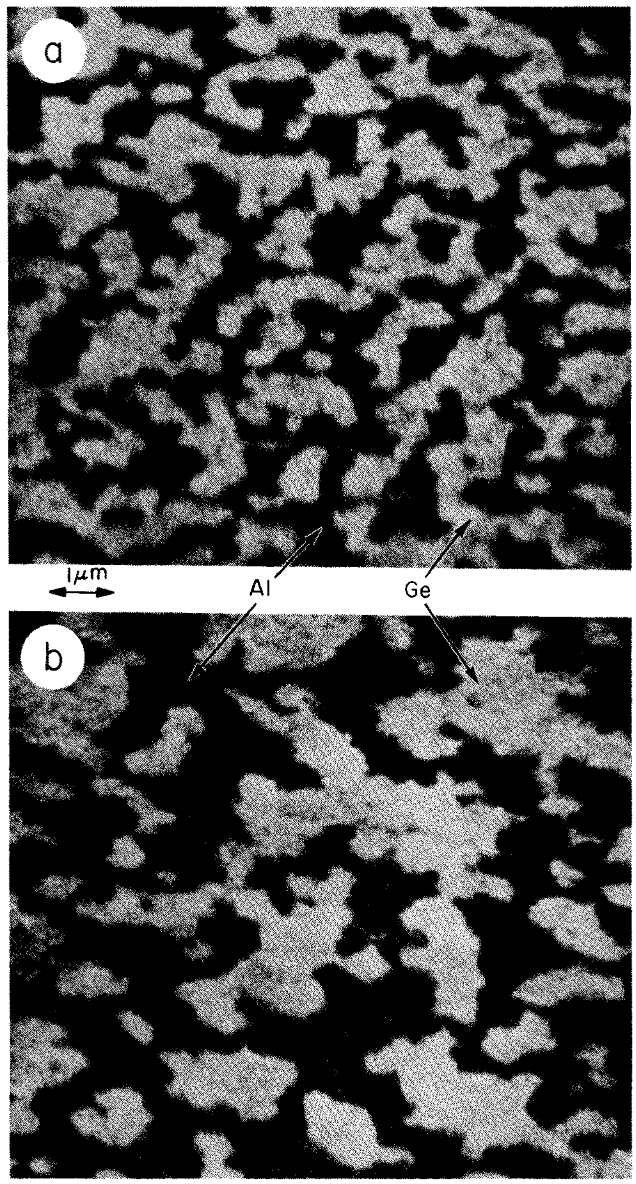

FIG. 7. Scanning electron micrographs at 10-keV electron energy of the sample shown in Fig. 6 after annealing at 300 °C for (a) 1 h and (b) 4 h. The identity of Al (black regions) and Ge (white regions) was determined by electron microprobe analysis.

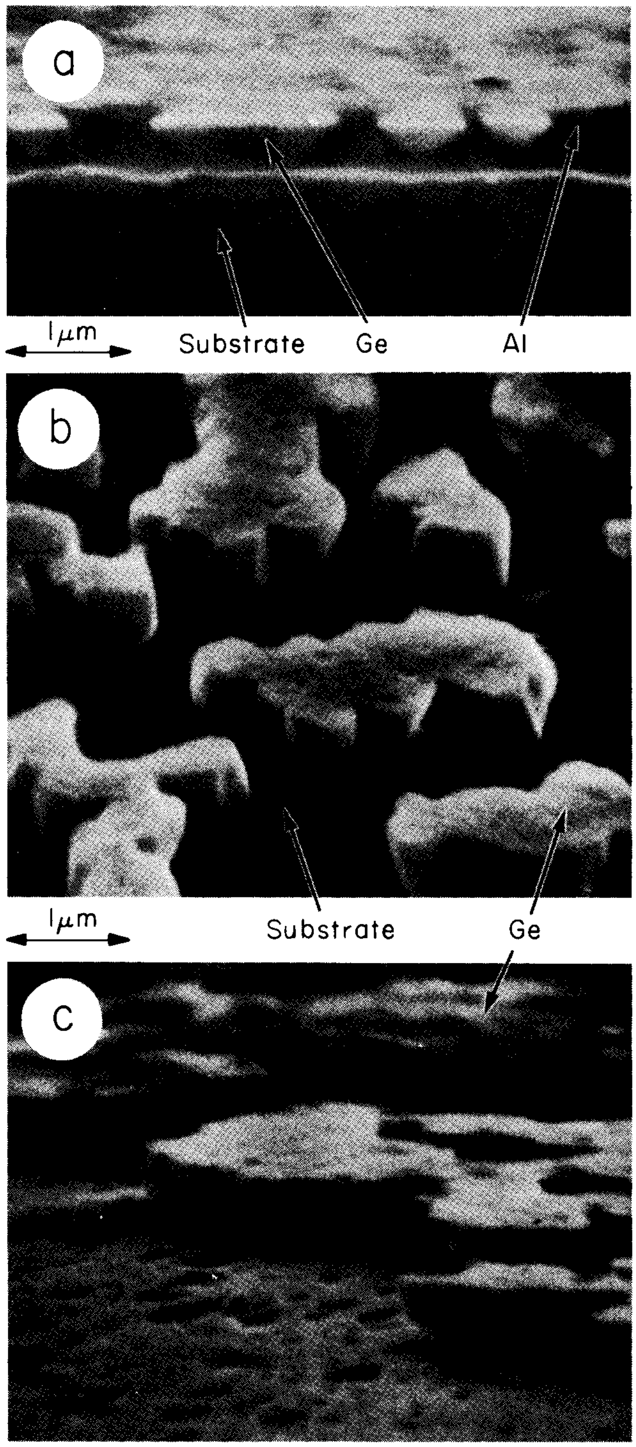

FIG. 8. Scanning electron micrographs at 10-keV electron energy of a Si substrate covered by 1840-Å Ge and 3600-Å Al and annealed at 300 °C for 1 h. (a) A cleaved surface taken with the electron beam incident at 80° off the surface normal. (b and c) The sample after removing the Al. In these cases the electron beam was incident at 65° and 85°, respectively.

substrate. This undercutting can be seen more clearly in Fig. 8(c), which is a micrograph taken at a greater angle of incidence to the surface.

Samples were also studied in a transmission electron microscope. Images of film stripped off the substrate after heat treatment again revealed that Ge precipitates were formed in the Al film. Furthermore, electron diffraction patterns clearly showed that the precipitates were crystalline in nature.[16]

B. Si/Ag

The Si/Ag system was studied with the same analytical tools as were used for the Ge/Al system. The results found are very similar to those just described in that the semiconductor crystallizes in the metal film. However, the range of temperatures in which the intermixing of the Si and the Ag films occurs is shifted to higher temperatures.

Figure 9 shows energy spectra from a Si substrate with 1670-Å Ag covered by 330-Å Si. The top spectrum in the figure shows the as-deposited case where there is a sharp Si peak (dotted area) with its high-energy edge at the energy corresponding to scattering from Si atoms at the surface. The high-energy edge of the Ag distribution (shaded area) is shifted to a lower energy owing to the overlaying Si layer. At lower energies (below 1 MeV) one can see the leading edge of the Si substrate continuum. Heat treatment at 300 °C for 240 min showed no significant changes in the spectrum. However, after heating at 400 °C for 180 min, a dramatic change was observed. The lower portion of Fig. 9 shows that the Si component had spread to lower energies, which corresponds to a motion of Si atoms into the Ag film. Also,

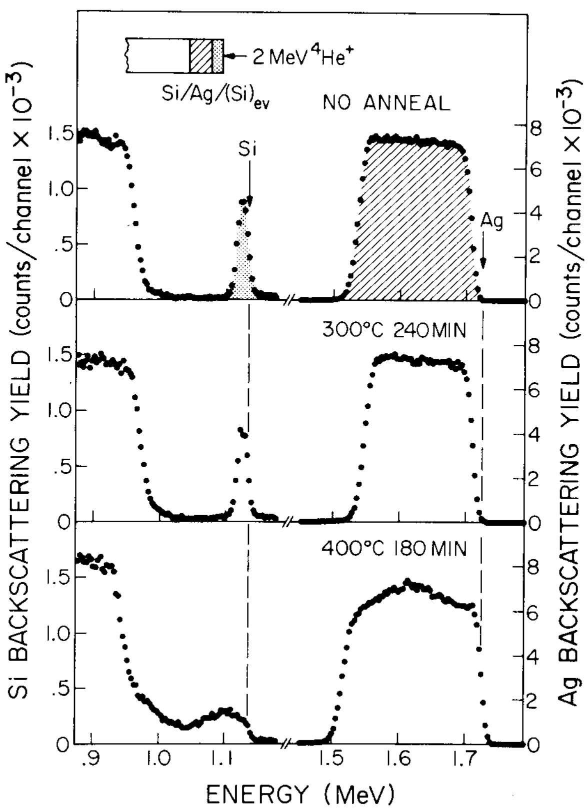

FIG. 9. Backscattering spectra for a Si substrate with 1670 Å of Ag covered by 330 Å of Si. The upper portion shows the as-deposited case, while the lower portions show spectra following anneals at 300 and 400 °C. As is indicated by the right-hand scale, the Ag yield is reduced by a factor of 5. The arrows indicate the energy corresponding to scattering from atoms at the surface.

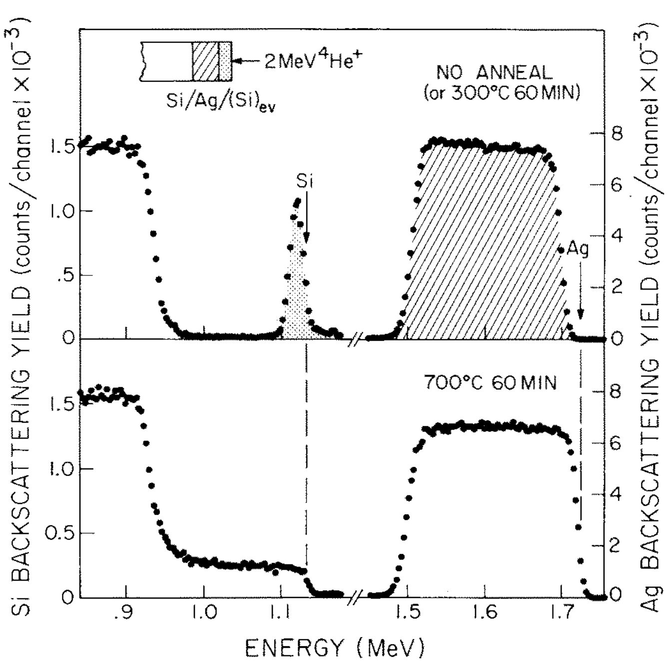

FIG. 10. Spectra for a Si substrate with 1900-Å Ag covered by 400-Å Si. The upper portion shows the as-deposited case. Comparison between this spectrum and one taken after annealing at 300 °C indicates that there was no change in the distribution of Ag and Si. The lower portion shows a spectrum after annealing at 700 °C for 1 h. The arrows indicate the energy corresponding to scattering from atoms at the surface.

the Ag component became wider and its high-energy edge shifted to the energy position of the surface. The shape of the Si and Ag spectra indicated, as is explained in the Appendix, that the Si and Ag were nonuniformly distributed throughout the composite film structure.

Figure 10 shows backscattering spectra from another specimen consisting of a Si substrate with 1900-Å Ag covered by 400-Å Si. The top spectrum of the figure shows the as-deposited case. As has been remarked before, heat treatment at 300 °C does not cause any significant change in the structure. Annealing at 700 °C for 60 min showed a mixing of Si and Ag to form a composite film. In comparison with the results after annealing at 400 °C (Fig. 9), the Si and Ag components in the 700 °C case of Fig. 10 are "flat". This shows that both Si and Ag are uniformly distributed in depth throughout the composite film. It is also worth noting that the Ag signal had steep edges after heat treatment, which demonstrates that the width of composite structure is uniform over the 2×2-mm beam.

Scanning electron micrographs of the same samples are presented in Fig. 11. The top view [Fig. 11(a)] is of the Si/Ag sample heated at 400 °C for 180 min (same sample as that in the lower spectrum in Fig. 9). The Ag matrix has been etched away in the left-hand portion, which leaves the Si precipitates exposed. Here the precipitates have a fine network appearance. The lower view [Fig. 11(b)] is of the Si/Ag sample heated at 700 °C for 60 min (same sample as that in the lower spectrum in Fig. 10), where the Ag matrix has been completely dissolved. Here the structure of the Si precipitates is much coarser than that in the previous sample. It was found to be a general feature that heating at high temperatures and for longer times produced larger precipitates than heating at lower temperatures and for shorter times. Scanning electron micrographs of cleaved

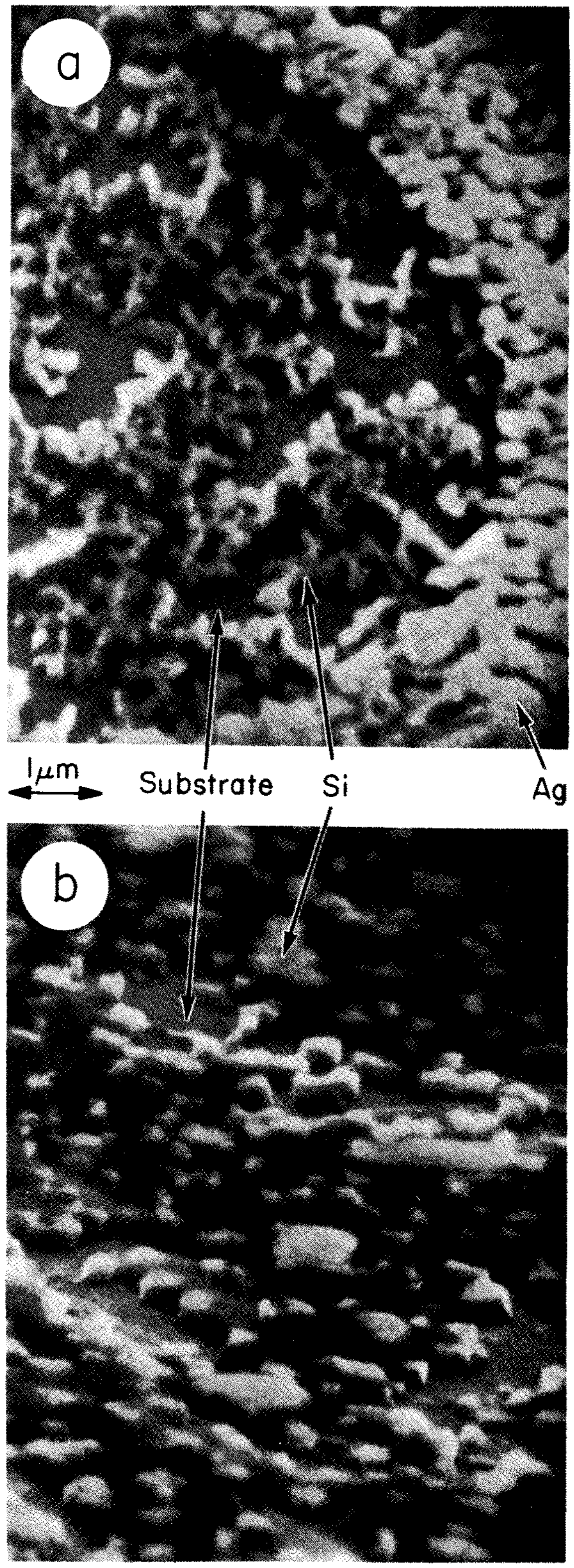

FIG. 11. Scanning electron micrographs of Si/Ag samples in which the Ag matrix has been etched away: (a) annealed at 400 °C for 180 min (same sample as that in Fig. 9); (b) annealed at 700 °C for 60 min (same samples as those in Fig. 10).

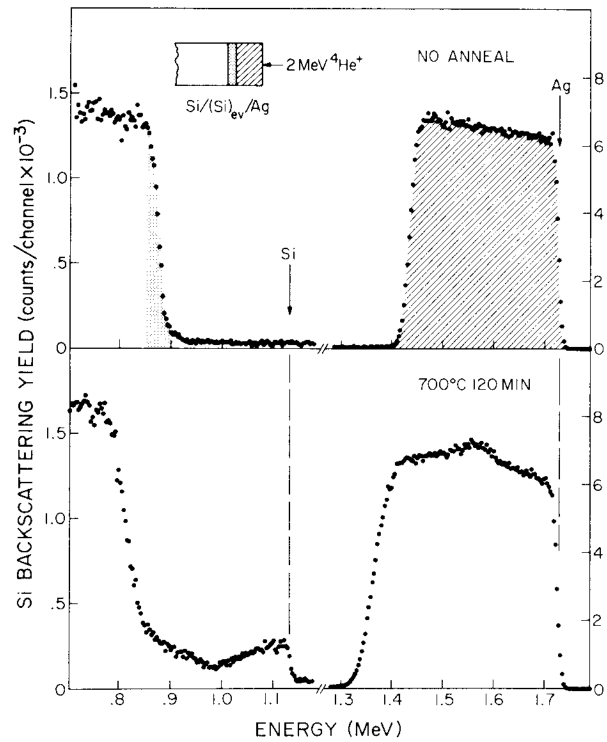

FIG. 12. Spectra for a Si substrate covered by 400-Å Si covered by 3000-Å Ag. The upper portion shows the as-deposited spectrum, and the lower portion shows the spectrum after annealing at 700 °C for 2 h. The arrows indicate the energy corresponding to scattering from atoms at the surface.

samples show that the Si precipitates reach through the whole composite film and thus are in contact with the Si substrate.

In the previously described Si/Ag samples the sequence of evaporation was such that the Ag was initially in contact with the substrate with the Si overlaying the Ag film. The opposite structure with Si in contact with the substrate covered by Ag was also studied. The backscattering spectrum for the as-deposited specimen is shown in Fig. 12. The component from the evaporated Si cannot be resolved from the Si substrate contribution and is indicated by the dotted area on the higher-energy edge of the Si spectrum. After heat treatment at 700 °C for 120 min, the backscattering spectrum has changed, as is apparent from the lower portion of Fig. 12. The top of the Ag component is not "flat", and the contribution from Si in the film is increasing towards the surface position. The shape of the spectrum indicates that there is a higher proportion of Si near the surface of the composite structure than there is at the substrate interface where the Si was initially deposited. The shapes of the signals from Si and Ag can be explained by the shape of the precipitates shown in Fig. 13 for the same sample. The precipitates appearing as islands on the Si substrate are fairly flat topped and show some undercutting near the interface. This tapered profile is the cause of the nonuniformities seen in the backscattering spectrum (see the Appendix).

Electron microprobe measurements on the Si/Ag sample showed that Si was located as localized precipitates in the composite film. Transmission electron diffraction analysis revealed that the precipitates were crystalline. This is discussed in paper II.

V. SUMMARY

We have studied the behavior of amorphous Si and Ge in contact with metal layers. The Si/Ag and Ge/Al cases were chosen as representative of simple eutectic systems. A wide range of experimental techniques were used: scanning electron microscopy, MeV He ion backscattering, electron microprobe analysis, and transmission electron diffraction. Taken together, experimental data utilizing these techniques lead to a consistent description.

Of the many reaction paths one can imagine to carry the amorphous semiconductor into its lowest-energy state—i.e., the crystalline state—we find a particularly simple path to be operative in the systems we have investigated. This path consists of dissolution of the amorphous Si or Ge into the adjacent solid metal film, diffusion, and growth of semiconductor crystallites out of the metal solution.

Energetically, the driving force for this isothermal dissolution and crystallite growth is provided by the higher free energy of the amorphous material, compared with that of the crystalline material. Kinetically, the metal layer provides the necessary solvent medium for the easy reaction path just described.

ACKNOWLEDGMENTS

SEM was carried out by J. Devaney of the Jet Propulsion Laboratories. The authors thank W.K. Chu for assistance in stopping power calculations. The advice and assistance of C.A. Barnes with nursing the Kellogg accelerator was invaluable.

APPENDIX

Helium ions incident at energy E_0 scatter from surface atoms through an angle θ_L with energy K^2E_0 and

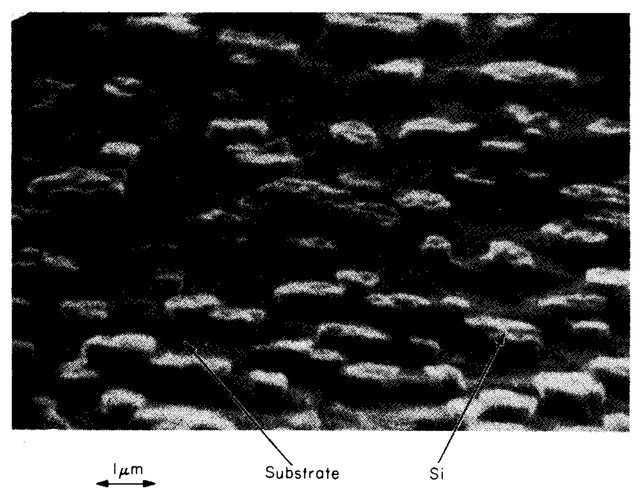

FIG. 13. Scanning electron micrograph of the sample shown in Fig. 12 with the Ag layer etched away. The 10-keV electron beam was incident at 80° off the surface normal.

TABLE I. Parameters used in the analysis of backscattering spectra of single elements for 2-MeV ^{4}He ions and $\theta_L = 170°$ (Ref. 22).

	Al	Si	Ge	Ag
K^2	0.552	0.566	0.803	0.863
ϵ [eV(10^{15} atoms/cm^2)$^{-1}$]	47	49.3	69.5	91.2
$[S]$ (eV/Å) [a]	51.5	46.1	57.9	104.1
σ (counts) [b]	13.3	15.5	83.7	181.1
Yield [c]	1	1.07	4.12	6.50

[a]Based on densities of 6.02×10^{22} Al atoms/cm^3, 4.98×10^{22} Si atoms/cm^3, 4.43×10^{22} Ge atoms/cm^3 and 5.85×10^{22} Ag atoms/cm^3.

[b]For convenience, σ is given as the number of counts from 10^{16} atoms/cm^2, a 1-μC dose of He ions, and a detector solid angle of 1 msr.

[c]Normalized to a scattering yield of unity for Al.

from atoms at a depth t below the surface with energy $K^2E_0 - t[S]$, where

$$[S] = K^2 \frac{dE}{dx}\bigg|_{E_0} + \frac{1}{\cos\theta_L}\frac{dE}{dx}\bigg|_{K^2E_0}$$

provides a conversion from energy loss to depth scale ($dE/dx = N\epsilon$, where ϵ is the stopping cross section per atom in eV cm^2 and N is the number of atoms per cm^3). Values of K^2, ϵ, and $[S]$ for various targets are given in Table I. The calculations for the depth scale $[S]$ are based on a linear approximation where it is assumed that $\epsilon \approx$ const over the inward and outward trajectories.

Table I also gives values for the scattering cross section σ for the target elements used in this study. The yield is the height Y of the spectrum (see Fig. 1 or 14) in counts per channel. The yield Y is proportional to $\sigma N/[S]$. The calculated values for these parameters are given in Table I and were used to calculated the relative yield values.

Figure 14 shows schematic spectra for a composite Si/Ag film on carbon and silicon substrates. Figure 14(a) [presented previously in Fig. 1(c)] is for equal atoms/cm^2 of Ag and Si on a carbon substrate. The backscattering components from the two species are clearly separated and have ratios of energy widths ($\Delta E_{Si}/\Delta E_{Ag} = 0.44$) and heights given by scattering cross sections, stopping powers, and exposed areas of the individual elements. In the present work, the geometrical configuration of the islands and the scattering angle are such that the majority of particles have inward and outward trajectories in one or the other of the two components of the target.

With a carbon substrate, the contribution from the low-mass substrate does not interfere with those from the overlying film. This is not the case when the substrate is of the same material as one of the constituents in the film. In Fig. 14(b) the spectrum is for the same Si and Ag film but on a Si substrate. The Ag signal is not affected. The Si signal has a step with a component at high energy owing to the Si in the film (dotted area) and at low energies owing to Si in the substrate (checked area). The width of the Si step is misleading and in this case is approximately twice that of ΔE_{Si}. This occurs because the $[S]$ factor in Ag is approximately twice that of Si (Table I). The contribution from the Si substrate under the Ag is shifted lower in energy than is the contribution from the substrate under Si.

A somewhat more complicated situation is shown in Fig. 14(c). In this case the Si islands are separated from the substrates with equal numbers of Si and Ag atoms/cm^2 and a thickness of the Si island two-thirds that of the film. There are two components to the Ag signal: One (cross hatched) indicates the region which extends from the surface to the substrate interface, and the other (shaded) indicates the region which lies between the Si islands and the substrate. The widths of these two signals correspond to the thicknesses of the two components (~3/1), and the heights correspond to the ratio of exposed area of Ag to the total film area. The Si signal has three components: The signal at high energy (dotted area) corresponds to the silicon islands, the step (checked area) corresponds to the portion of the substrate underneath the Si islands, and the unshaded area corresponds to the Si substrate. The width of the dotted area corresponds to the thickness of the Si islands, and the height corresponds to the area of the islands.

Figure 15 shows schematic spectra for composite Ge/Al films on carbon, Si, and Ge substrates. Figure 15(a) represents a situation with a carbon substrate. The two

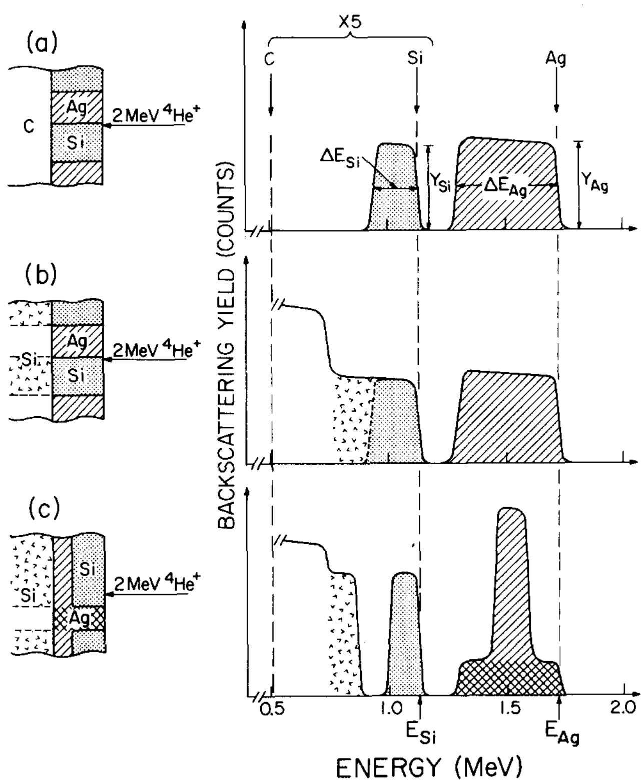

FIG. 14. Schematic energy spectra for 2-MeV ^{4}He ions backscattered from equal numbers of Si and Ag atoms/cm^2 in composite structures on carbon and Si substrates. (a) Spectrum for a Si film deposited on a Ag film; (b) spectrum for a uniform mixture; (c) spectrum for elemental islands. The arrows indicate the energy corresponding to scattering from atoms at the surface.

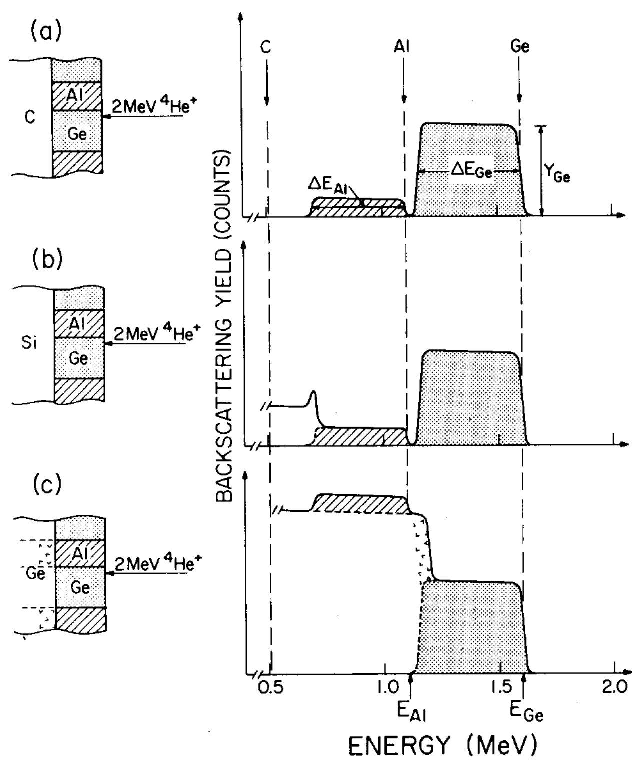

FIG. 15. Schematic energy spectra for 2-MeV ^{4}He ions backscattered from equal numbers of Ge and Al atoms/cm^2 in elemental islands on (a) carbon, (b) Si, and (c) Ge substrates. The arrows indicate the energy corresponding to scattering from atoms at the surface.

signals from Al and Ge are clearly resolved. In Fig. 15(b) a Si substrate is used. The Ge signal is still separated, but the low-energy edge of the Al signal interferes with the Si signal to form an overlap peak due to the different masses of Si and Al.[21] In Fig. 15(c), the Ge substrate gives a thick-target continuum up to ~1.2 MeV. On this continuum the Al signal is superimposed. Owing to differences in the stopping power of Ge and Al, the step in the spectrum of high energies is again misleading and does not directly correspond to the energy loss in the Ge islands, which are wider than this step (dotted area).

*Work supported in part by the Office of Naval Research.

[1]P.A. Totta and R.P. Sopher, IBM J. Res. Dev. 13, 226 (1969).
[2]J.O. McCaldin and H. Sankur, Appl. Phys. Lett. 19, 524 (1971).
[3]T. Oki, Y. Ogawa, and Y. Fujiki, Jap. J. Appl. Phys. 8, 1056 (1969).
[4]J.R. Bosnell and U.C. Voisey, Thin Solid Films 6, 161 (1970).
[5]S. Herd, P. Chaudhari, and M.H. Brodsky, J. Non-Crystal. Solids 7, 309 (1972).
[6]D.H. Lee, R.R. Hart, and O.J. Marsh, Appl. Phys. Lett. 20, 73 (1972).
[7]U. Koster, Acta Metall. 20, 1361 (1972).
[8]M.H. Brodsky and D. Turnbull, Bull. Am. Phys. Soc. 16, 304 (1971).
[9]A. Hiraki, E. Lugujjo, and J.W. Mayer, J. Appl. Phys. 43, 3643 (1972).
[10]J.M. Caywood, Met. Trans. 4, 735 (1973).
[11]H. Sankur, J.O. McCaldin, and J. Devaney, Appl. Phys. Lett. 22, 64 (1973).
[12]V. Marrello, J.M. Caywood, J.W. Mayer, and M-A. Nicolet, Phys. Status Solidi A 13, 531 (1972).
[13]J.O. McCaldin and H. Sankur, Appl. Phys. Lett. 20, 171 (1972).
[14]A.N. Rossalimo and D. Turnbull, Acta Metall. 21, 21 (1973).
[15]D. Sigurd, G. Ottaviani, V. Marrello, J.W. Mayer, and J.O. McCaldin, J. Non-Crystal. Solids 12, 135 (1973).
[16]D. Sigurd, G. Ottaviani, H. Arnal, and J.W. Mayer, following paper, J. Appl. Phys. 45, 1740 (1974).
[17]T.M. Donovan, E.J. Ashley, and W.E. Spicer, Phys. Lett. A 32, 85 (1970).
[18]T.M. Donovan, Ph.D. thesis (Stanford University, 1970) (unpublished).
[19]M-A. Nicolet, J.W. Mayer, and I.V. Mitchell, Science 177, 841 (1972).
[20]J.F. Ziegler and W.-K. Chu (private communication).
[21]I.V. Mitchell, M. Kamoshida, and J.W. Mayer, J. Appl. Phys. 42, 4378 (1971).
[22]J.F. Ziegler and W.-K. Chu, Thin Solid Films 19, 281 (1973).